Chiral Three-Nucleon Interactions in Light Nuclei, Neutron-α Scattering, and Neutron Matter

J. E. Lynn, I. Tews, J. Carlson, S. Gandolfi, A. Gezerlis, K. E. Schmidt, and A. Schwenk

Phys. Rev. Lett. **116**, 062501 — Published 9 February 2016

DOI: 10.1103/PhysRevLett.116.062501

Chiral Three-Nucleon Interactions in Light Nuclei, Neutron-α Scattering, and Neutron Matter

J. E. Lynn,[1,*] I. Tews,[2,3] J. Carlson,[1] S. Gandolfi,[1] A. Gezerlis,[4] K. E. Schmidt,[5] and A. Schwenk[2,3]

[1] *Theoretical Division, Los Alamos National Laboratory, Los Alamos, New Mexico 87545, USA*
[2] *Institut für Kernphysik, Technische Universität Darmstadt, 64289 Darmstadt, Germany*
[3] *ExtreMe Matter Institute EMMI, GSI Helmholtzzentrum für Schwerionenforschung GmbH, 64291 Darmstadt, Germany*
[4] *Department of Physics, University of Guelph, Guelph, Ontario, N1G 2W1, Canada*
[5] *Department of Physics, Arizona State University, Tempe, Arizona 85287, USA*

We present quantum Monte Carlo calculations of light nuclei, neutron-α scattering, and neutron matter using local two- and three-nucleon (3N) interactions derived from chiral effective field theory up to next-to-next-to-leading order (N^{2}LO). The two undetermined 3N low-energy couplings are fit to the ^{4}He binding energy and, for the first time, to the spin-orbit splitting in the neutron-α P-wave phase shifts. Furthermore, we investigate different choices of local 3N operator structures and find that chiral interactions at N^{2}LO are able to simultaneously reproduce the properties of $A = 4, 5$ systems and of neutron matter, in contrast to commonly used phenomenological 3N interactions.

PACS numbers: 21.60.–n, 21.10.–k, 21.30.–x, 21.60.De

Three-nucleon (3N) interactions are essential for a reliable prediction of the properties of light nuclei and nucleonic matter [1–5]. In quantum Monte Carlo (QMC) calculations phenomenological 3N interactions such as the Urbana [6] and Illinois [7] models have been used with great success [3, 8]. However, such models suffer from certain disadvantages: They are not based on a systematic expansion and it was found that the Illinois forces tend to overbind neutron matter [9, 10]. It is therefore unlikely that these phenomenological models can be used to correctly predict the properties of heavy neutron-rich nuclei.

An approach which addresses these shortcomings is chiral effective field theory (EFT) [2, 11–14]. Chiral EFT is a low-energy effective theory consistent with the symmetries of quantum chromodynamics and provides a systematic expansion for nuclear forces. It includes contributions from long-range pion-exchange interactions explicitly and expands the short-distance interactions into a systematic set of contact operators accompanied by low-energy couplings fit to experimental data. Chiral EFT enables the determination of theoretical uncertainties and systematic order-by-order improvement; for recent work see Refs. [15–18].

Chiral EFT also predicts consistent many-body interactions. In Weinberg power-counting, 3N forces first enter at next-to-next-to-leading order (N^{2}LO) [19, 20] and contain three contributions: a two-pion-exchange interaction V_C, a one-pion-exchange-contact interaction V_D and a 3N contact interaction V_E. While the first is accompanied by the couplings c_i from the pion-nucleon sector, the latter two are accompanied by the couplings c_D and c_E which have to be determined in $A > 2$ systems.

In addition to systematic nuclear forces, reliable many-body methods are required to describe properties of light nuclei and to determine the properties of dense neutron matter. QMC methods, which solve the many-body Schrödinger equation stochastically, are such a class of methods. Both the Green's function Monte Carlo (GFMC) method and the auxiliary-field diffusion Monte Carlo (AFDMC) method rely on projection in imaginary time τ,

$$\lim_{\tau\to\infty} \mathrm{e}^{-H\tau} \left|\Psi_T\right\rangle \to \left|\Psi_0\right\rangle , \tag{1}$$

with H the Hamiltonian of the system, and $|\Psi_T\rangle$ a trial wave function not orthogonal to the many-body ground state $|\Psi_0\rangle$. For a recent review of developments and applications of QMC in nuclear physics, see Ref. [3]. Recently, we have developed chiral EFT interactions for QMC calculations [21–24], which provide nonperturbative results for testing the chiral expansion scheme [22] and benchmarks for neutron matter up to high density [21, 23]. However, these studies were limited to two-nucleon (NN) interactions only or to an exploratory study of neutron matter with only the long-range parts of the 3N interaction.

In this Letter, we include consistent 3N interactions at N^{2}LO in coordinate space [24] in GFMC calculations of light nuclei and n-α scattering, and AFDMC calculations of neutron matter. We fit the two couplings c_D and c_E to the ^{4}He binding energy and low-energy n-α scattering P-wave phase shifts. The latter system has been studied using various approaches, see for example Refs. [25–27]. These observables are expected to be less correlated than fits to structure properties of $A = 3, 4$ systems because the spin-orbit and $T = \frac{3}{2}$ components of the 3N interaction enter directly.

In phenomenological 3N models, any short-range parts which arise from the Fourier transformation of pion exchanges are typically absorbed into other short-distance structures: we retain these explicitly. We choose the 3N cutoff $R_{3\mathrm{N}} = R_0$, where R_0 is the NN cutoff, and vary the cutoff in the range $R_0 = 1.0 - 1.2$ fm [21–24]. Note that with a finite cutoff certain ambiguities appear including

the specific operator form associated with the shorter-range interactions. In the Fourier transformation of V_D two possible operator structures arise:

$$V_{D1} = \frac{g_A c_D m_\pi^2}{96\pi\Lambda_\chi F_\pi^4} \sum_{i<j<k} \sum_{\rm cyc} \boldsymbol{\tau}_i \cdot \boldsymbol{\tau}_k \left[X_{ik}(\mathbf{r}_{kj})\delta_{R_{3N}}(\mathbf{r}_{ij}) + X_{ik}(\mathbf{r}_{ij})\delta_{R_{3N}}(\mathbf{r}_{kj}) - \frac{8\pi}{m_\pi^2}\boldsymbol{\sigma}_i \cdot \boldsymbol{\sigma}_k \delta_{R_{3N}}(\mathbf{r}_{ij})\delta_{R_{3N}}(\mathbf{r}_{kj}) \right], \quad (2a)$$

$$V_{D2} = \frac{g_A c_D m_\pi^2}{96\pi\Lambda_\chi F_\pi^4} \sum_{i<j<k} \sum_{\rm cyc} \boldsymbol{\tau}_i \cdot \boldsymbol{\tau}_k \left[X_{ik}(\mathbf{r}_{ik}) - \frac{4\pi}{m_\pi^2}\boldsymbol{\sigma}_i \cdot \boldsymbol{\sigma}_k \delta_{R_{3N}}(\mathbf{r}_{ik}) \right] \left[\delta_{R_{3N}}(\mathbf{r}_{ij}) + \delta_{R_{3N}}(\mathbf{r}_{kj}) \right], \quad (2b)$$

where $X_{ik}(\mathbf{r}) = [S_{ik}(\mathbf{r})\,T(r) + \boldsymbol{\sigma}_i \cdot \boldsymbol{\sigma}_k]Y(r)$ is the coordinate-space pion propagator, $S_{ik}(\mathbf{r}) = 3\boldsymbol{\sigma}_i \cdot \hat{\mathbf{r}}\boldsymbol{\sigma}_k \cdot \hat{\mathbf{r}} - \boldsymbol{\sigma}_i \cdot \boldsymbol{\sigma}_k$ is the tensor operator, and the tensor and Yukawa functions are defined as $T(r) = 1 + 3/(m_\pi r) + 3/(m_\pi r)^2$ and $Y(r) = \mathrm{e}^{-m_\pi r}/r$. The smeared-out delta function $\delta_{R_{3N}}(\mathbf{r}) = \frac{1}{\pi\Gamma(3/4)R_{3N}^3}\mathrm{e}^{-(r/R_{3N})^4}$ and the long-range regulator multiplying Y, $f_{\rm long}(r) = 1 - \mathrm{e}^{-(r/R_{3N})^4}$ are consistent with the choices made in the NN interaction [21–24]. The sum $i < j < k$ runs over all particles 1 to A, and the cyclic sum runs over the cyclic permutations of a given triple.

The two possible V_D structures agree in the limit of $R_{3N} \to 0$, because the delta functions then enforce $i = j$ ($k = j$) in the first (second) term, in which case Eqs. (2a) and (2b) would coincide. The V_D interaction does not distinguish which of the two nucleons in the contact participates in the pion exchange. The second choice V_{D2} can be obtained with the exchange of a fictitious heavy scalar particle between the two nucleons in the contact. This ambiguity was also pointed out in [28]. The differences between Eqs. (2a) and (2b) are regulator effects and therefore higher order in the chiral expansion, but it is important to investigate how they affect different observables at this order.

Similar effects arise in the 3N contact interaction V_E. Here, the main ambiguity is the choice of the 3N contact operator. The same Fierz-rearrangement freedom that allows for a selection of (mostly) local contact operators in the NN sector up to N^{2}LO exists in the 3N sector at this order. Symmetry considerations allow the choice of one of the following six operators [20]:

$$\begin{aligned} &\{\mathbb{1}, \boldsymbol{\sigma}_i \cdot \boldsymbol{\sigma}_j, \boldsymbol{\tau}_i \cdot \boldsymbol{\tau}_j, \boldsymbol{\sigma}_i \cdot \boldsymbol{\sigma}_j \boldsymbol{\tau}_i \cdot \boldsymbol{\tau}_j, \\ &\boldsymbol{\sigma}_i \cdot \boldsymbol{\sigma}_j \boldsymbol{\tau}_i \cdot \boldsymbol{\tau}_k, [(\boldsymbol{\sigma}_i \times \boldsymbol{\sigma}_j) \cdot \boldsymbol{\sigma}_k][(\boldsymbol{\tau}_i \times \boldsymbol{\tau}_j) \cdot \boldsymbol{\tau}_k]\}. \end{aligned} \quad (3)$$

The usual choice is $\boldsymbol{\tau}_i \cdot \boldsymbol{\tau}_j$. Here, we investigate two other choices: first with the operator $\mathbb{1}$, and second with a projector operator $\mathcal{P}$ on to triples with $S = \frac{1}{2}$ and $T = \frac{1}{2}$:

$$\mathcal{P} = \frac{1}{36}\Big(3 - \sum_{i<j} \boldsymbol{\sigma}_i \cdot \boldsymbol{\sigma}_j\Big)\Big(3 - \sum_{k<\ell} \boldsymbol{\tau}_k \cdot \boldsymbol{\tau}_\ell\Big), \quad (4)$$

where the sums are over pairs in a given triple. In the infinite-momentum cutoff limit only these $S = \frac{1}{2}, T = \frac{1}{2}$ triples would contribute to V_E due to the Pauli principle. Thus, in the following we will explore three possible structures:

$$V_{E\tau} = \frac{c_E}{\Lambda_\chi F_\pi^4} \sum_{i<j<k} \sum_{\rm cyc} \boldsymbol{\tau}_i \cdot \boldsymbol{\tau}_k \delta_{R_{3N}}(\mathbf{r}_{kj})\delta_{R_{3N}}(\mathbf{r}_{ij}), \quad (5a)$$

$$V_{E\mathbb{1}} = \frac{c_E}{\Lambda_\chi F_\pi^4} \sum_{i<j<k} \sum_{\rm cyc} \delta_{R_{3N}}(\mathbf{r}_{kj})\delta_{R_{3N}}(\mathbf{r}_{ij}), \quad (5b)$$

$$V_{E\mathcal{P}} = \frac{c_E}{\Lambda_\chi F_\pi^4} \sum_{i<j<k} \sum_{\rm cyc} \mathcal{P}\,\delta_{R_{3N}}(\mathbf{r}_{kj})\delta_{R_{3N}}(\mathbf{r}_{ij}). \quad (5c)$$

We stress that there are more possible operator structures for V_D and V_E, which will be investigated in future work.

Having specified all 3N structures, we vary the values of the couplings c_D and c_E to fit the ^{4}He binding energy as shown in Fig. 1a. We display curves for V_{D1} and V_{D2} using $V_{E\tau}$ and both cutoffs $R_0 = 1.0$ fm and $R_0 = 1.2$ fm. In addition, we show curves for V_{D2} using the other two possible V_E structures and the cutoff $R_0 = 1.0$ fm. For all of these possibilities, the stars give the values for the couplings which also fit P-wave n-α scattering phase shifts as shown in Fig. 1b. The resulting couplings c_D and c_E are given in Table I. In all cases $\langle V_E \rangle$ is repulsive in ^{4}He except for the case with $(D2, E\tau)$ with the softer cutoff ($R_0 = 1.2$ fm), where it is mildly attractive.

For $R_0 = 1.0$ fm and $V_{E\tau}$, $c_D \approx 0$ and both forms of V_D simultaneously fit the ^{4}He binding energy and P-wave n-α scattering phase shifts (see Fig. 1b). However, in the softer-cutoff case $R_0 = 1.2$ fm, V_{D1} and V_{D2} lead to different couplings. For V_{D1}, the splitting between the two P waves appears to saturate in c_D for values of $c_D > 2$, e.g., the $P\ \frac{3}{2}^-$ phase shift for $c_D = 2.0,\ 3.0,$ and 5.0 at $E_{\rm cm} = 1.3$ MeV are each ∼75 deg., which is ∼35 deg. below the R-matrix value. Since we cannot fit the P-wave n-α scattering phase shifts in this case (V_{D1} and $R_0 = 1.2$ fm) we do not consider it in the following. Instead for V_{D2} and $R_0 = 1.2$ fm, the splitting can be fit, as is evident from Fig. 1b. For V_{D2} using $V_{E\mathbb{1}}$ or $V_{E\mathcal{P}}$ and $R_0 = 1.0$ fm, both the ^{4}He binding energy and the P-wave n-α scattering phase shifts can be simultaneously fit: we show only the case with $V_{E\mathcal{P}}$ in Fig. 1b. There we also show the NLO results which are a clear indication that 3N

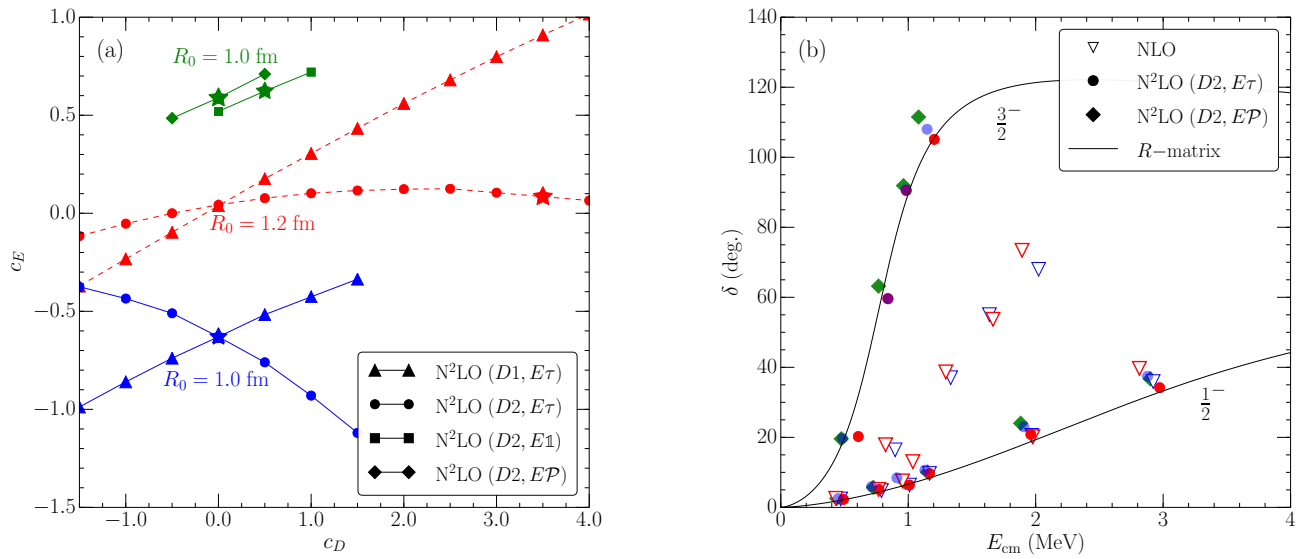

FIG. 1. (color online). (a) Couplings c_E vs. c_D obtained by fitting the ^{4}He binding energy for different 3N-operator forms. Triangles are obtained by using V_{D1} and $V_{E\tau}$ while the other symbols are obtained for V_{D2} and three different V_E-operator structures. Blue and green lines (lower and upper) correspond to $R_0 = 1.0$ fm, while red lines (central) correspond to $R_0 = 1.2$ fm. The GFMC statistical errors are smaller than the symbols. The stars correspond to the values of c_D and c_E which simultaneously fit the n-α P-wave phase shifts (see Table I and right panel). No fit to both observables can be obtained for the case with $R_0 = 1.2$ fm and V_{D1}. (b) P-wave n-α elastic scattering phase shifts compared with an R-matrix analysis of the data. Colors and symbols correspond to the left panel. We also include phase shifts calculated at NLO, which clearly indicate the necessity of 3N interactions to fit the P-wave splitting.

TABLE I. Fit values for the couplings c_D and c_E for different choices of 3N forces and cutoffs.

V_{3N}	R_0 (fm)	c_E	c_D
N^{2}LO ($D1, E\tau$)	1.0	−0.63	0.0
	1.2	–	–
N^{2}LO ($D2, E\tau$)	1.0	−0.63	0.0
	1.2	0.09	3.5
N^{2}LO ($D2, E\mathbb{1}$)	1.0	0.62	0.5
N^{2}LO ($D2, E\mathcal{P}$)	1.0	0.59	0.0

forces are necessary to properly describe n-α scattering. Similar results have been found in Ref. [29–31]. Because $A = 3, 4$ systems are largely insensitive to odd-parity partial waves, we find no significant dependence on the choice of structures in V_D. However, our results in n-α P-wave scattering show a substantial sensitivity: V_{D1} appears to have a smaller effect than V_{D2}.

In Fig. 2, we show ground-state energies and point-proton radii for $A = 3, 4$ nuclei at NLO and N^{2}LO using V_{D2} and $V_{E\tau}$ for $R_0 = 1.0$ fm and $R_0 = 1.2$ fm in comparison with experiment. The ground-state energies of the $A = 3$ systems compare well with experimental values. The ground-state energy of ^{4}He is used in fitting c_D and c_E, and so is forced to match the experimental value to within ≈ 0.03 MeV. The point-proton radii also compare well with values extracted from experiment. The theoretical uncertainty at each order is estimated through the expected size of higher-order contributions, see Ref. [32] for details. We include results from LO, NLO, and N^{2}LO in the analysis using the Fermi momentum and the pion mass as the small scales for neutron matter and nuclei, respectively. The error bars presented here are comparable to those shown in Ref. [33], although it is worth emphasizing that our calculations represent a complete estimate of the uncertainty at N^{2}LO since we include 3N interactions. Other choices for 3N structures give similar results.

It is noteworthy that NN and 3N interactions derived from chiral EFT up to N^{2}LO have sufficient freedom such that n-α scattering phase shifts in Fig. 1b and properties of light nuclei in Fig. 2 can be simultaneously described. The failures of the Urbana IX model in underbinding nuclei and underpredicting the spin-orbit splitting in neutron-rich systems including the n-α system were among the factors motivating the addition of the three-pion exchange diagrams in the Illinois of 3N models [7]. Our results show that chiral 3N forces at N^{2}LO,

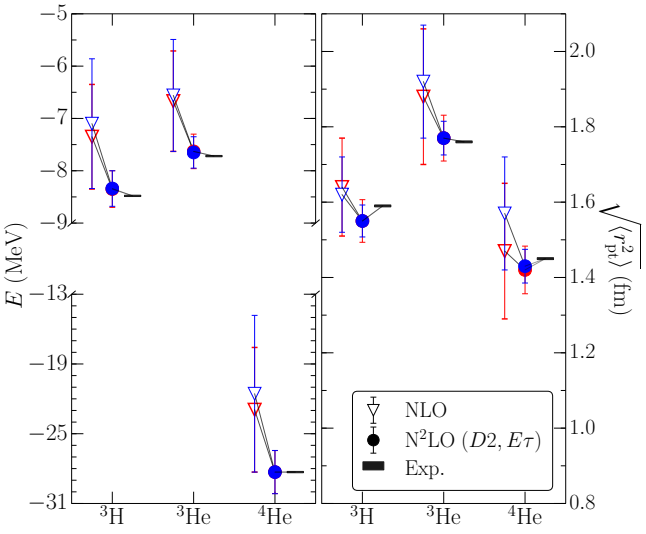

FIG. 2. (color online). Ground-state energies and point proton radii for $A = 3, 4$ nuclei calculated at NLO and N^{2}LO (with V_{D2} and $V_{E\tau}$) compared with experiment. Blue (red) symbols correspond to $R_0 = 1.0$ fm ($R_0 = 1.2$ fm). The errors are obtained as described in the text and also include the GFMC statistical uncertainties.

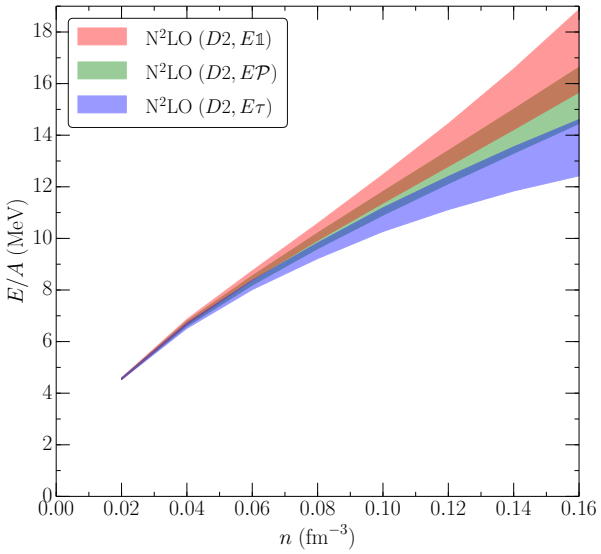

FIG. 3. (color online). The energy per particle in neutron matter as a function of density for the NN and full 3N interactions at N^{2}LO with $R_0 = 1.0$ fm. We use V_{D2} and different 3N contact structures: the blue band corresponds to $V_{E\tau}$, the red band to $V_{E\mathbb{1}}$ and the green band to $V_{E\mathcal{P}}$. The green band coincides with the NN+2π-exchange-only result because both V_D and V_E vanish in this case. The bands are calculated as described in the text.

including the shorter-range parts in the pion exchanges, allow the simultaneous fit. These interactions should be tested further in light p-shell nuclei.

Finally, we study the full chiral N^{2}LO forces, including all 3N contributions, in neutron matter to extend the results from Ref. [24]. More specifically, we examine the effects of different V_D and V_E structures on the equation of state of neutron matter. Although these terms vanish in the limit of infinite cutoff, they contribute for finite cutoffs. In Fig. 3 we show results for the neutron matter energy per particle as a function of the density calculated with the AFDMC method as described in Refs. [3, 34, 35]. We show the energies for $R_0 = 1.0$ fm for the NN and full 3N interactions. We use V_{D2} and the three different V_E structures: $V_{E\tau}$ (blue band), $V_{E\mathbb{1}}$ (red band), and $V_{E\mathcal{P}}$ (green band). The error bands are determined as in the light nuclei case. The $V_{E\mathcal{P}}$ interaction fits $A = 4, 5$ with a vanishing c_D, hence this choice of V_E leads to an equation of state identical to the equation of state with NN + V_C as in Ref. [24] (the projector $\mathcal{P}$ is zero for pure neutron systems) and qualitatively similar to previous results using chiral interactions at N^{2}LO [36] and N^{3}LO [37].

As discussed, the contributions of V_D and V_E are only regulator effects for neutrons. However, they are sizable and result in a larger error band. At saturation density $n_0 \sim 0.16$ fm^{-3} the difference of the central value of the energy per neutron after inclusion of the 3N contacts $V_{E\mathbb{1}}$ or $V_{E\tau}$ is $\sim$2 MeV, leading to a total error band with a range of $\sim$6.5 MeV when considering different V_E structures. This relatively large uncertainty can be qualitatively explained when considering the following effects. Because the expectation value $\langle \sum_{i<j} \boldsymbol{\tau}_i \cdot \boldsymbol{\tau}_j \rangle$ has a sign opposite to that of the expectation value $\langle \mathbb{1} \rangle$ in ^{4}He, c_E will also have opposite signs in the two cases to fit the binding energy. However, in neutron matter both operators are the same, spreading the uncertainty band. A similar argument was made in Ref. [38].

With the regulators used here, the Fierz-rearrangement invariance valid at infinite cutoff is only approximate at finite cutoff, and hence the different choices of V_D and V_E can lead to different results. The different local structures can lead to finite relative P-wave contributions. These can be eliminated by choosing $V_{E\mathcal{P}}$, which has a projection onto even-parity waves (predominantly S waves). The usual nonlocal regulator in momentum-space does not couple S and P waves.

In conclusion, we find for the first time that chiral interactions can simultaneously fit light nuclei and low-energy P-wave n-α scattering and provide reasonable estimates for the neutron matter equation of state. Other

commonly used phenomenological 3N models do not provide this capability. These chiral forces should be tested in light p-shell nuclei, medium-mass nuclei, and isospin-symmetric nuclear matter to gauge their ability to describe global properties of nuclear systems.

We also find that the ambiguities associated with contact-operator choices can be significant when moving from light nuclei to neutron matter and possibly to medium-mass nuclei where the $T = \frac{3}{2}$ triples play a more significant role. The reason for the sizable impact may be the regulators used here, which break the Fierz-rearrangement invariance, making further investigations of regulator choices a priority. The impact of these ambiguities in the contact operators can contribute to the uncertainties and needs to be studied further.

We thank G. Hale for useful discussions and for providing us with the R-matrix analysis of the n-α phase shifts. We also thank A. Dyhdalo, E. Epelbaum, R. J. Furnstahl, K. Hebeler, and A. Lovato for useful discussions. This work was supported by the NUCLEI SciDAC program, the U.S. DOE under contract DE-AC52-06NA25396, the ERC Grant No. 307986 STRONGINT, the Natural Sciences and Engineering Research Council of Canada, the LANL LDRD program, and the NSF under grant PHY-1404405. Computational resources have been provided by Los Alamos Open Supercomputing and the Jülich Supercomputing Center. We also used resources provided by NERSC, which is supported by the US DOE under Contract DE-AC02-05CH11231.

* E-mail: joel.lynn@gmail.com

[1] N. Kalantar-Nayestanaki, E. Epelbaum, J. G. Messchendorp, and A. Nogga, Rept. Prog. Phys. **75**, 016301 (2012).
[2] H.-W. Hammer, A. Nogga, and A. Schwenk, Rev. Mod. Phys. **85**, 197 (2013).
[3] J. Carlson, S. Gandolfi, F. Pederiva, S. C. Pieper, R. Schiavilla, K. E. Schmidt, and R. B. Wiringa, Rev. Mod. Phys. **87**, 1067 (2015).
[4] K. Hebeler, J. D. Holt, J. Menendez, and A. Schwenk, Ann. Rev. Nucl. Part. Sci. **65**, 457 (2015).
[5] S. Gandolfi, A. Gezerlis, and J. Carlson, Annu. Rev. Nucl. Part. Sci. **65**, 303 (2015).
[6] B. S. Pudliner, V. R. Pandharipande, J. Carlson, S. C. Pieper, and R. B. Wiringa, Phys. Rev. C **56**, 1720 (1997).
[7] S. C. Pieper, V. R. Pandharipande, R. B. Wiringa, and J. Carlson, Phys. Rev. C **64**, 014001 (2001).
[8] S. C. Pieper, Riv. Nuovo Cimento **31**, 709 (2008).
[9] A. Sarsa, S. Fantoni, K. E. Schmidt, and F. Pederiva, Phys. Rev. C **68**, 024308 (2003).
[10] P. Maris, J. P. Vary, S. Gandolfi, J. Carlson, and S. C. Pieper, Phys. Rev. C **87**, 054318 (2013).
[11] S. Weinberg, Phys. Lett. **B251**, 288 (1990).
[12] S. Weinberg, Nucl. Phys. **B363**, 3 (1991).
[13] E. Epelbaum, H.-W. Hammer, and U.-G. Meißner, Rev. Mod. Phys. **81**, 1773 (2009).
[14] R. Machleidt and D. R. Entem, Phys. Rep. **503**, 1 (2011).
[15] E. Epelbaum, H. Krebs, and U.-G. Meißner, Phys. Rev. Lett. **115**, 122301 (2015).
[16] A. Ekström, G. R. Jansen, K. A. Wendt, G. Hagen, T. Papenbrock, B. D. Carlsson, C. Forssén, M. Hjorth-Jensen, P. Navrátil, and W. Nazarewicz, Phys. Rev. C **91**, 051301 (2015).
[17] B. D. Carlsson, A. Ekström, C. Forssén, D. F. Strömberg, O. Lilja, M. Lindby, B. A. Mattsson, and K. A. Wendt, arXiv:1506.02466.
[18] R. J. Furnstahl, N. Klco, D. R. Phillips, and S. Wesolowski, Phys. Rev. C **92**, 024005 (2015).
[19] U. van Kolck, Phys. Rev. C **49**, 2932 (1994).
[20] E. Epelbaum, A. Nogga, W. Glöckle, H. Kamada, U.-G. Meißner, and H. Witała, Phys. Rev. C **66**, 064001 (2002).
[21] A. Gezerlis, I. Tews, E. Epelbaum, S. Gandolfi, K. Hebeler, A. Nogga, and A. Schwenk, Phys. Rev. Lett. **111**, 032501 (2013).
[22] J. E. Lynn, J. Carlson, E. Epelbaum, S. Gandolfi, A. Gezerlis, and A. Schwenk, Phys. Rev. Lett. **113**, 192501 (2014).
[23] A. Gezerlis, I. Tews, E. Epelbaum, M. Freunek, S. Gandolfi, K. Hebeler, A. Nogga, and A. Schwenk, Phys. Rev. C **90**, 054323 (2014).
[24] I. Tews, S. Gandolfi, A. Gezerlis, and A. Schwenk, (2015), arXiv:1507.05561.
[25] K. M. Nollett, S. C. Pieper, R. B. Wiringa, J. Carlson, and G. M. Hale, Phys. Rev. Lett. **99**, 022502 (2007).
[26] G. Hagen, D. J. Dean, M. Hjorth-Jensen, and T. Papenbrock, Phys. Lett. **B656**, 169 (2007).
[27] S. Quaglioni and P. Navratil, Phys. Rev. Lett. **101**, 092501 (2008).
[28] P. Navrátil, Few-Body Systems **41**, 117 (2007).
[29] G. Hupin, J. Langhammer, P. Navrátil, S. Quaglioni, A. Calci, and R. Roth, Phys. Rev. C **88**, 054622 (2013).
[30] G. Hupin, S. Quaglioni, and P. Navrátil, Phys. Rev. C **90**, 061601 (2014).
[31] S. Quaglioni, G. Hupin, J. Langhammer, C. Romero-Redondo, M. D. Schuster, C. W. Johnson, P. Navrátil, and R. Roth, JPS Conf. Proc. **6**, 010022 (2015).
[32] E. Epelbaum, H. Krebs, and U. G. Meiner, Eur. Phys. J. **A51**, 53 (2015).
[33] S. Binder *et al.*, arXiv:1505.07218.
[34] S. Gandolfi, A. Y. Illarionov, K. E. Schmidt, F. Pederiva, and S. Fantoni, Phys. Rev. C **79**, 054005 (2009).
[35] S. Gandolfi, J. Carlson, and S. Reddy, Phys. Rev. C **85**, 032801 (2012).
[36] G. Hagen, T. Papenbrock, A. Ekström, K. A. Wendt, G. Baardsen, S. Gandolfi, M. Hjorth-Jensen, and C. J. Horowitz, Phys. Rev. C **89**, 014319 (2014).
[37] I. Tews, T. Krüger, K. Hebeler, and A. Schwenk, Phys. Rev. Lett. **110**, 032504 (2013).
[38] A. Lovato, O. Benhar, S. Fantoni, and K. E. Schmidt, Phys. Rev. C **85**, 024003 (2012).